2B2-3

Arrival Angle Distribution Control in MIMO-OTA Measurement Environment Using Double-Layered Reverberation Chamber

Ichiro Oshima [1], Yoshio Karasawa [2]
[1] Denki Kogyo Co., Ltd.
13-4 Satsuki-cho, Kanuma-shi, Tochigi 322-0014, Japan, E-mail: i-oshima@denkikogyo.co.jp
[2] Advanced Wireless Communication Research Center (AWCC),
The University of Electro-Communications (UEC Tokyo)
1-5-1 Chofugaoka, Chofu-shi, Tokyo 182-8585, Japan, E-mail: karasawa@ee.uec.ac.jp

1. Introduction

Two types of methods are used to develop MIMO-OTA (over-the-air) measurement systems. One is a fading emulator based method that involves the arrangement of a number of actual radiation antennas that represent scattering objects. The other involves the use of a radio echoic chamber named "reverberation chamber" (RC) consisting of six metallic walls [1]. An RC has the advantage of being able to easily create a multipath-rich environment with large delay. On the other hand, it is incapable of controlling the propagation parameters and producing fast temporal variations. A pioneering example of an RC system has been presented [2]; however, we consider that this system has limited capability. Therefore, we developed a new RC and suggested approaches to overcome the demerits of the previously proposed RC [3]. In this paper, we have proposed an RC with arrival angle distribution control; further, through an experiment, we demonstrated that channel characteristics corresponding to desired angular distributions can be achieved using this RC.

2. Structure of double-layered reverberation chamber

2.1 Basic structure

Figure 1 shows the double-layered RC that controls the arrival angle distribution. The outer chamber is made of six aluminum plates, and the dimensions of the chamber are 4 m × 2 m × 2 m. The inner chamber has the shape of an octagonal prism, and it consists of a top plate, a bottom plate, and eight side walls made of aluminum. The prism has a diameter and height of 1 m each. In the side walls, apertures are drilled in a periodic pattern. The transmitting antenna is placed in the outer chamber but outside the inner chamber, and the receiving antenna is placed at the center of the inner chamber.

2.2 Side wall design of inner reverberation chamber

Figure 2 shows the periodic square apertures in the side walls of the inner chamber. These apertures operate as a frequency selective surface, and the dimensions and the interval of each square aperture are determined such that the aperture allows the transmission of a frequency of 5.1 GHz, which is the frequency used in our experiment. The aperture dimensions and interval obtained via a simulation are 30 mm × 30 mm and 45 mm, respectively. At the center of each aperture, metallic elements with a width of 3 mm and a length of l [mm] are placed on a glass epoxy substrate; these elements are termed reflective elements. The transmission amplitude of a vertically polarized wave is controlled by the length of these elements. Further, inside the side walls, λ/4-type radio wave absorbers are embedded. These absorbers attenuate multiple reflections inside the inner chamber. Figure 3 shows the simulation result of the transmission loss when a vertically polarized plane wave is incident on the side wall. The transmission loss is approximately 4 dB in the absence of reflective elements (l = 0 mm); the transmission loss increases with an increase in the length of the elements, and it is maximized at l = 22.5 mm. Using the abovementioned structure, we expect that the arrival angle distribution determined by the transmission amplitude of the wave incident on the side walls is achieved at the receiving antenna side.

2.3 Setting of transmission angle

As shown in Fig. 4, the apertures in the area of the side walls from where the incident wave is transmitted do not possess reflective elements (i.e., l = 0 mm), and the apertures in the area from where the incident wave is blocked possess reflective elements of length l = 22.5 mm. The central angle of arrival of the wave is $\theta = 90°$, and the value of the transmission angle 2ϕ is varied. Here, the transmission angles are selected as 45°, 135°, and 360°, which correspond to the side walls one, three, and eight of the inner chamber, respectively. The two-dimensional spatial correlation in the x direction at the receiving antenna side $\rho_a(\Delta x)$ is expressed by the following equation:

$$\rho_a(\Delta x) = \frac{\int_0^{2\pi} \Omega(\theta) e^{jk\Delta x \cos\theta} d\theta}{\int_0^{2\pi} \Omega(\theta) d\theta}, \quad (1)$$

where $\Omega(\theta)$ represents the angular distribution. We estimated the value of the angular distribution by comparing the measured spatial correlation to the theoretical spatial correlation.

3. Experiment

3.1 Spatial correlation characteristics and cumulative distribution of received power level

The measurement conditions to study the spatial correlation characteristics are as follows. A 45° polarized dipole antenna is used as the transmitting antenna and a vertically polarized dipole antenna is used as the receiving antenna. The receiving antenna is fixed on the slide rail and is moved from the inside center of the inner chamber to a distance x = 200 mm with a step of 2 mm (101 points); the propagation characteristics are measured at each point using a network analyzer. Further, the measuring frequency is 5.0~5.2 GHz with 1,601 sweep points.

First, we measured the correlation coefficient of received power variation at each point with respect to the power at the center. Figure 5 shows the spatial correlation characteristics for transmission angles 2ϕ of 45°, 135°, and 360°. In this figure, the theoretical spatial correlations of uniform and Laplacian distributions are also shown; here, the interval of the uniform distribution and the angular spread of Laplacian distribution are the same as the transmission angle. The main lobe in the spatial correlation characteristics spreads gradually with a reduction in the transmission angle, and the measured correlation becomes similar to that of Laplacian distribution.

Next, we investigated the cumulative probability distribution of the received power level. In Fig.6, the statistical data for transmission angles of 45° and 360° are shown. We can observe that the measured distributions follow a Rayleigh distribution, irrespective of the transmission angle.

3.2 Eigenvalue distribution of 4 × 4 MIMO antenna array

Finally, we examine the eigenvalue distribution to determine whether the channel characteristics corresponding to angular distribution are achieved using a 4 × 4 MIMO antenna array. Sleeve antennas are used for both the transmitting and receiving antennas, and these antennas are linear array antennas in the x direction. The array distances of the transmitting and receiving antennas are 1.5λ and 0.5λ, respectively. We measured each channel characteristic without moving the receiving antennas spatially, and the measurements were performed at a frequency of 5.0~5.2 GHz with 16,001 sweep points.

Figure 7 shows the cumulative probability distributions of the eigenvalues for transmission angles of 45°, 135°, and 360°. The measured data were normalized to the mean value of the received power. Simulated data were obtained using the Kronecker model, where the spatial correlation of the transmitting antenna was not considered because of its large array distance, whereas that of the receiving antenna was calculated using eq.(1). In addition, the angular distributions at the receiving antenna side followed a Laplacian distribution. The measured and simulated distributions exhibit a similar behavior. Therefore, it is found that channel characteristics corresponding to the desired arrival angle distributions are achieved.

4. Conclusion

We presented a double-layered reverberation chamber as a MIMO-OTA system with arrival angle distribution control. We demonstrated the design of the side walls of the inner chamber to

control the transmission amplitude and the setting of the transmission angle. We measured the spatial correlation characteristics and found that the arrival wave distribution is similar to Laplacian distribution, whose angular spread is the same as the transmission angle. On the basis of the measured eigenvalue distribution of a 4 × 4 MIMO antenna array, we demonstrated that the channel characteristics corresponding to the desired arrival angle distributions were achieved.

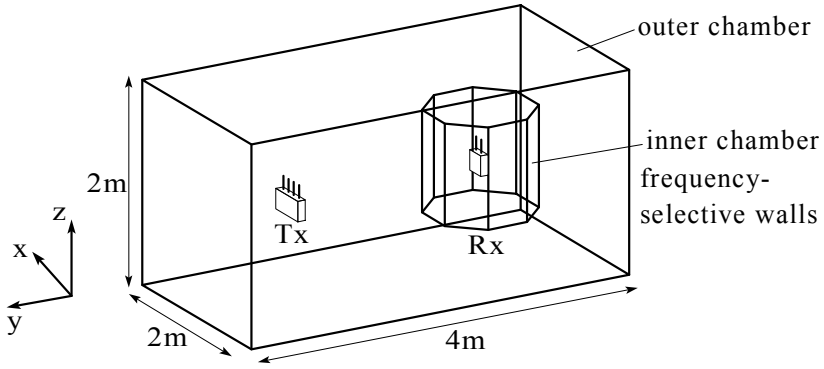

Figure 1: Structure of double-layered reverberation chamber.

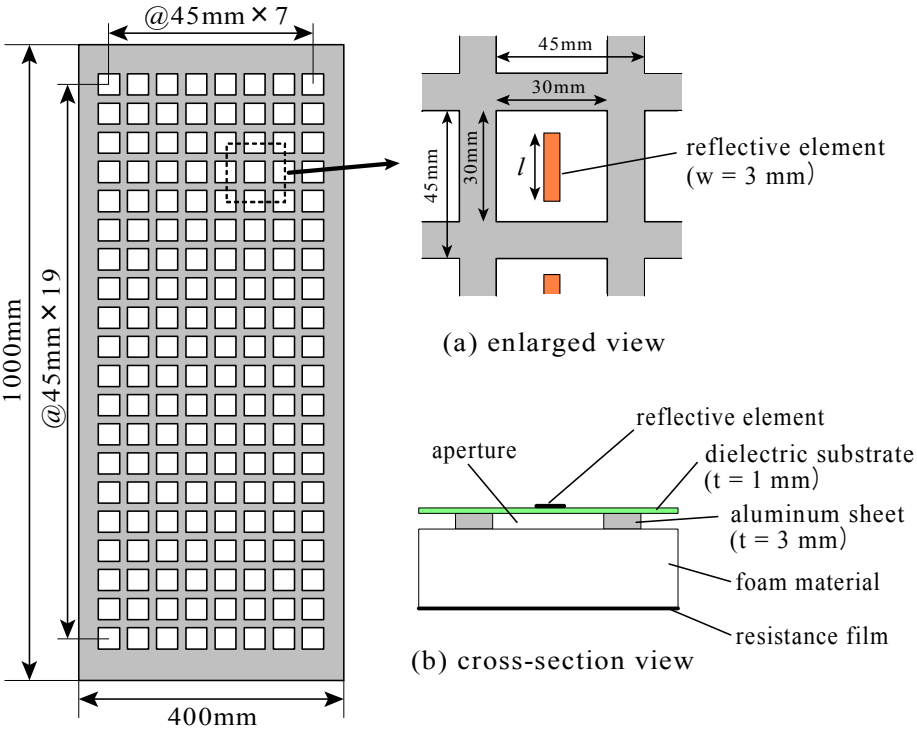

Figure 2: Structure of side wall to control arrival angle distribution.

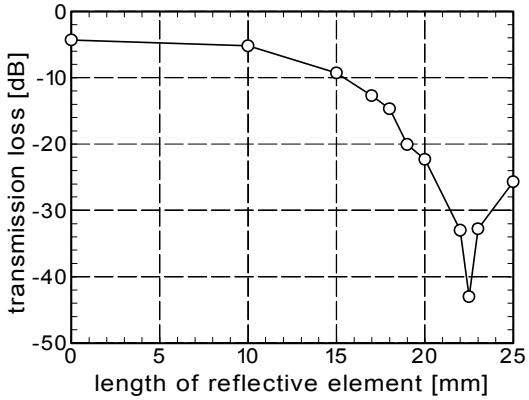

Figure 3: Transmission loss in case of normal incidence of 5.1 GHz plane wave.

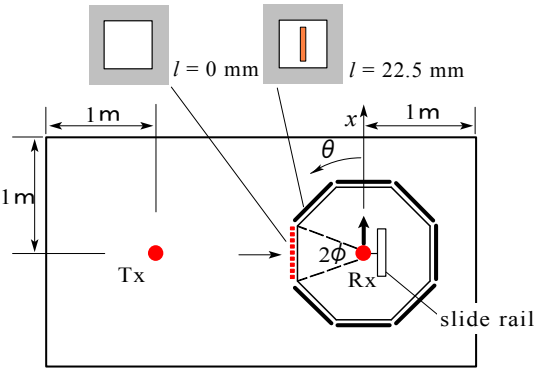

Figure 4: Setting of transmission angle (top view).

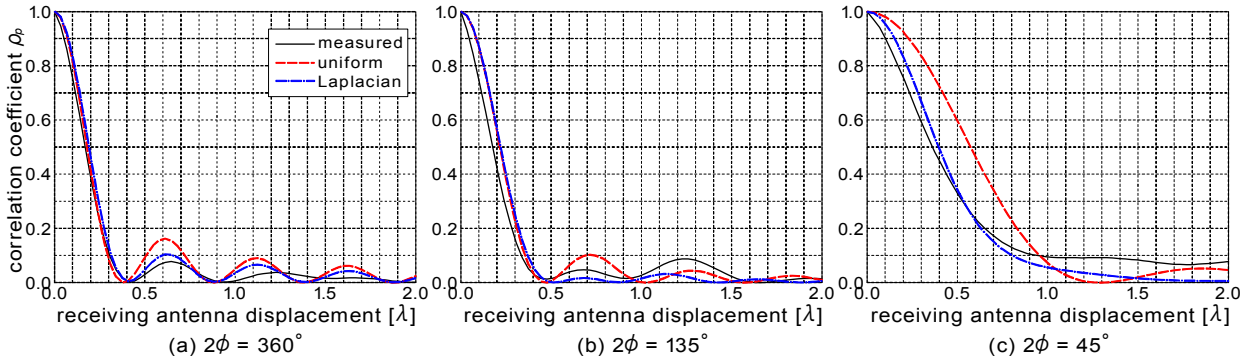

Figure 5: Spatial correlation for each transmission angle.

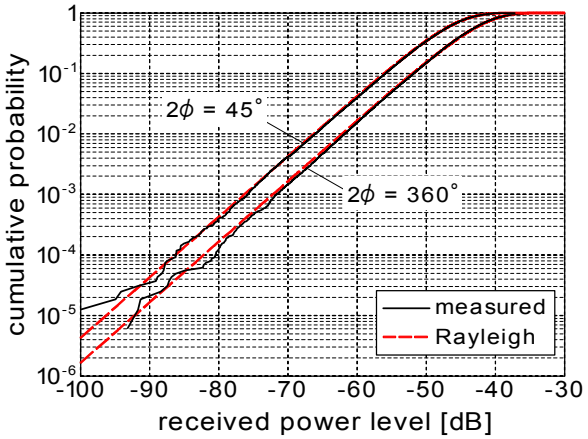

Figure 6: Cumulative probability distribution of received power level.

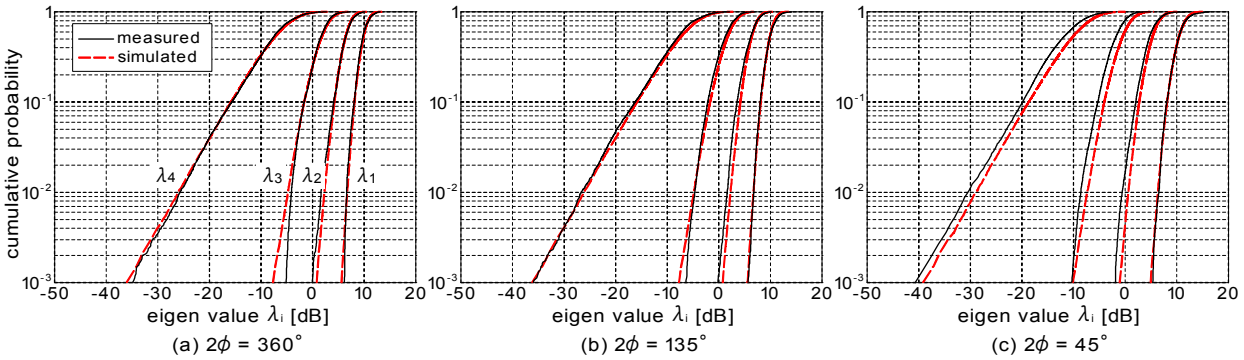

Figure 7: Eigenvalue distribution of 4 × 4 MIMO antenna array for each transmission angle.

References

[1] 3GPP TR37.976 v1.1.0, "Measurement of radiated performance for MIMO and multi-antenna reception for HSPA and LTE terminals (Release 10)."

[2] P.S. Kildal and K. Rosengren, "Correlation and capacity of MIMO systems and mutual coupling radiation efficiency, and diversity gain of their antennas: Simulation and measurements in a reverberation chamber," IEEE Commun. Mag., vol.42, no.12, pp.104-111, Dec. 2004.

[3] I. Oshima and Y. Karasawa, "Control of multipath propagation environment by using double-layered reverberation chamber," IEICE Trans. Commun. (Japanese edition), vol.J94-B, no.9, pp.1056-1064, Sept. 2011.